

## Observation of a crossover of $S_{2n}$ in the island of inversion from precision mass spectrometry

A. A. Kwiatkowski,<sup>1,\*</sup> C. Andreoiu,<sup>2</sup> J. C. Bale,<sup>1,3</sup> A. Chaudhuri,<sup>1</sup> U. Chowdhury,<sup>1,4</sup> S. Malbrunot-Ettenauer,<sup>1,5,†</sup> A. T. Gallant,<sup>1,5</sup> A. Grossheim,<sup>1</sup> G. Gwinner,<sup>4</sup> A. Lennarz,<sup>1,6</sup> T. D. Macdonald,<sup>1,5</sup> T. J. M. Rauch,<sup>1,7</sup> B. E. Schultz,<sup>1,‡</sup> S. Seeraji,<sup>2</sup> M. C. Simon,<sup>1,§</sup> V. V. Simon,<sup>1,8,9,||</sup> D. Lunney,<sup>10</sup> A. Poves,<sup>1,11</sup> and J. Dilling<sup>1,5</sup>

<sup>1</sup>TRIUMF, 4004 Wesbrook Mall, Vancouver, British Columbia V6T 2A3, Canada

<sup>2</sup>Department of Chemistry, Simon Fraser University, Burnaby, British Columbia V5A 1S6, Canada

<sup>3</sup>Department of Physics, Simon Fraser University, Burnaby, British Columbia V5A 1S6, Canada

<sup>4</sup>Department of Physics and Astronomy, University of Manitoba, Winnipeg, Manitoba R3T 2N2, Canada

<sup>5</sup>Department of Physics and Astronomy, University of British Columbia, Vancouver, British Columbia V6T 1Z1, Canada

<sup>6</sup>Institut für Kernphysik, Westfälische Wilhelms-Universität, 48149 Münster, Germany

<sup>7</sup>Friedrich-Alexander-Universität Erlangen-Nürnberg, 91054 Erlangen, Germany

<sup>8</sup>Max-Planck-Institut für Kernphysik, Saupfercheckweg 1, 69117 Heidelberg, Germany

<sup>9</sup>Fakultät für Physik und Astronomie, Ruprecht-Karls-Universität, 69120 Heidelberg, Germany

<sup>10</sup>CSNSM-IN2P3-CNRS, Université Paris 11, 91405 Orsay, France

<sup>11</sup>Departamento de Física Teórica and IFT-UAM/CSIC, Universidad Autónoma de Madrid, E-28049 Madrid, Spain

(Received 28 October 2014; revised manuscript received 2 October 2015; published 7 December 2015)

Mass measurements have been performed of the neutron-rich Al isotopes near  $N \approx 20$ , along the island of inversion. In general, the precision of the mass values was improved by an order of magnitude. Based on these new and more accurate data, we find the two-neutron separation energy of  $^{34}_{13}\text{Al}$  to be 24.8(10.8) keV less than that of  $^{33}_{12}\text{Mg}$ . This represents the first known crossover on the  $S_{2n}$  surface of the chart of nuclides. Large-scale shell-model calculations show that the crossover can be attributed to exceptionally large energy gains of the Mg isotopes in the island of inversion.

DOI: [10.1103/PhysRevC.92.061301](https://doi.org/10.1103/PhysRevC.92.061301)

PACS number(s): 21.10.Dr, 27.30.+t, 82.80.Qx

The structure of nuclei along the valley of stability is well described by the nuclear shell model [1], similar to the atomic equivalent, wherein particularly stable configurations occur at so-called magic numbers and other special properties such as spin and discontinuities in binding energies can be explained. The picture of immovable shell gaps first broke down in studies of neutron-rich nuclei around the magic neutron number  $N = 20$  in Na isotopes [2], where irregularities in the binding energy were observed. With the advent of rare-isotope-beam facilities [3], more detailed studies have become possible, and this and other anomalies in mean-square radii and nuclear spectra [4] have since been observed and attributed to strong deformation caused by an intruder configuration from the  $pf$  shell dropping below the normal  $sd$ -shell configuration [5].

The region around  $N = 20$ , now called the *island of inversion*, exhibits another unusual feature relating to the

two-neutron separation energy  $S_{2n}$ . Defined as the energy required to remove two neutrons, the  $S_{2n}$  is given by

$$S_{2n}(N, Z) = -M(N, Z) + M(N - 2, Z) + 2M_n, \quad (1)$$

where  $M(N, Z)$  is the atomic mass and  $M_n$  is the neutron mass. Typically the  $S_{2n}$  decreases steadily towards the neutron dripline, whereas changes in its trend indicate features such as shell closures and regions of unusual nuclear structure. When plotted as a function of neutron number, the  $S_{2n}$  values of the isotopic chains show a stunning regularity (see plots in Ref. [6], pp. 1827–1834). For  $^{34}\text{Al}$  and  $^{33}\text{Mg}$  at  $N = 21$ , however, the values overlap—an occurrence found nowhere else on the chart of nuclides thus far—as shown in Fig. 1. Until recently the uncertainties of their  $S_{2n}$  values were too large to exclude or confirm a crossover as they were determined predominantly by time-of-flight (TOF) mass measurements [7]. Albeit extremely fast ( $\sim \mu\text{s}$ ), this technique requires several calibrant nuclides, of which there are few candidates far from the valley of stability, and thus uncertainties can reach hundreds of keV. Since the  $S_{2n}$  value of a given nuclide requires its mass combined with that of an isotope with two less neutrons, the anomaly could be due to the mass values of  $^{31,33}\text{Mg}$  or  $^{32,34}\text{Al}$ . Recent direct mass measurements of  $^{31,33}\text{Mg}$  reported by our collaboration [8] eliminate them as the source of the problem. As the Al isotopes lay between the deformed Mg isotopes and the spherical Si isotopes [9], they play a critical role in understanding the intruder mechanism. In this Rapid Communication, we report new high-precision and accurate Penning-trap mass measurements of neutron-rich Al isotopes which demonstrate that the Al  $S_{2n}$  falls below that of Mg at  $N = 21$ . In addition, we performed large-scale shell-model

\*Present address: Cyclotron Institute and Department of Physics, Texas A & M University, College Station, TX 77843, USA; [aniak@triumf.ca](mailto:aniak@triumf.ca)

†Present address: CERN, Physics Department, 1211 Genève 23, Switzerland.

‡Present address: Department of Physics, University of Notre Dame, Notre Dame, IN 46556, USA.

§Present address: Stefan Meyer Institute for Subatomic Physics, Austrian Academy of Sciences, Boltzmannsgasse 3, 1090 Vienna, Austria.

||Present address: Physikalisches Institut, Universität Heidelberg, Im Neuenheimer Feld 226, 69120 Heidelberg, Germany.

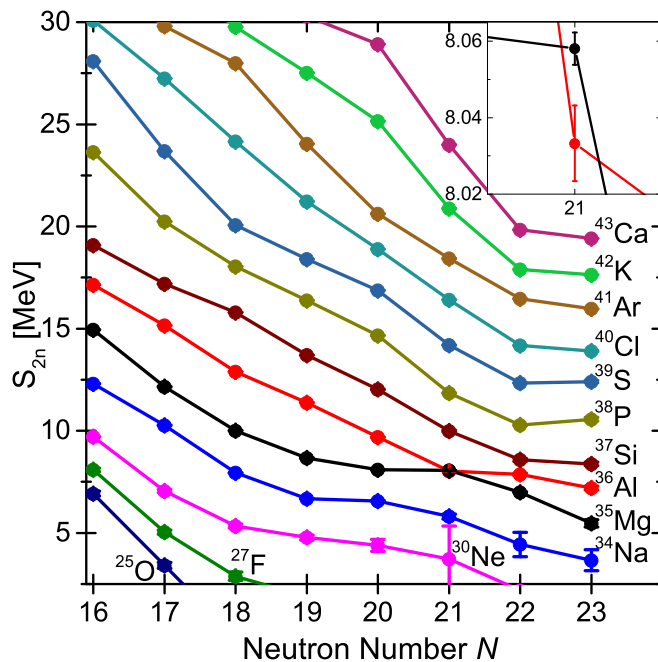


FIG. 1. (Color online) The two-neutron separation energy  $S_{2n}$  curves near the island of inversion. Data are taken from AME'12 [6] and this work. The difference between the two ( $\sim 100$  eV to 100 keV) is not visible on this scale. The inset displays the singular crossover at  $N = 21$ .

calculations which indicate correlation energy is the principal source of the crossover.

The mass measurements were performed at TRIUMF's Ion Trap for Atomic and Nuclear science (TITAN) Penning-trap facility [12]. Penning traps have been established as the tool of choice for mass measurements of accelerator-generated isotopes [13]. The TITAN system has been successfully used for fast mass measurements of singly and highly charged ions, including the halo nuclides  $^8\text{He}$  [14] and  $^{11}\text{Li}$  [15], the superallowed  $\beta$ -emitter  $^{74}\text{Rb}$  [16], and  $r$ -process nuclides including  $^{98}\text{Sr}$  [17]. The measurements herein were carried out in three experiments: first  $^{29,32}\text{Al}$ , second  $^{30,31,33,34}\text{Al}$  isotopes, and finally  $^{27}\text{Al}$  off line. In all cases, the radioactive beams were produced at the ISAC facility by bombarding  $\text{UC}_x$  targets with up to  $10\ \mu\text{A}$  of 500 MeV protons and ionized with resonant laser ionization [18]. The stable ions were produced off line:  $^{16}\text{O}_2^+$  in the Off-line Ion Source (OLIS) and  $^{23}\text{Na}^+$ ,  $^{27}\text{Al}^+$ , and  $^{39,41}\text{K}^+$  from TITAN's surface-ionization ion source. The ions were delivered to the TITAN radio-frequency quadrupole beam cooler and buncher [19], where the continuous beam was accumulated, cooled, and bunched. The ion bunches were then sent to the measurement Penning trap (MPET) [20] for the mass measurement. A fast time-of-flight mass filter [21] upstream of MPET was used to select the desired isobar. No isobaric contaminants were found in the beam.

The mass of the ion of interest was determined in the Penning trap by measuring the cyclotron frequency  $2\pi\nu_c = q/mB$ , where  $q/m$  is the charge-to-mass ratio of the ion and  $B$  is the magnetic field strength, using the time-of-flight ion-

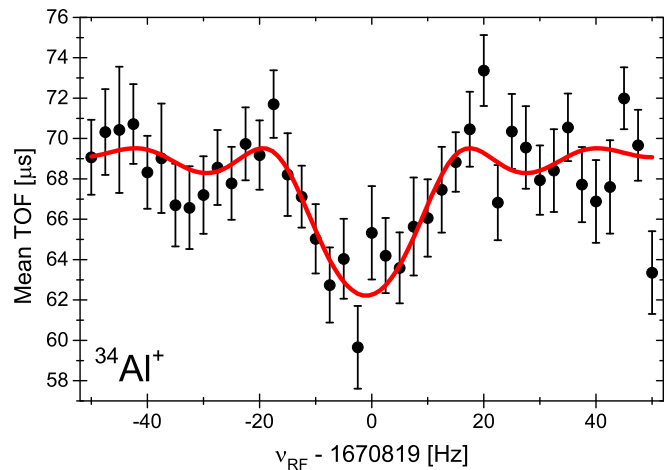


FIG. 2. (Color online) A TOF-ICR resonance of  $^{34}\text{Al}^+$  for an excitation time of 47 ms. The solid curve is an analytic fit [22] to the data.

cyclotron-resonance (TOF-ICR) [23,24] technique. A typical TOF resonance curve of  $^{34}\text{Al}^+$  is shown in Fig. 2. To calibrate the magnetic field, the cyclotron frequency of a reference ion ( $\text{O}_2^+$  or  $^{39}\text{K}^+$ ) with a well-known mass was measured, interleaved in time with measurements of the ion of interest. The magnetic field strength was linearly interpolated to the measurement time of Al ion. Therefore, the experimental result is the ratio of the cyclotron frequencies

$$R = \frac{\nu_{c,ref}}{\nu_{c,Al}} = \frac{m_{Al}}{m_{ref}}, \quad (2)$$

where the subscripts identify the singly charged reference or the Al ion. Table I lists the reference ion and frequency ratio measured for each Al isotope. For the unstable Al isotopes, the statistical uncertainties on the ratio  $\delta R/R$  were between  $2$  and  $20 \times 10^{-8}$ . Systematic uncertainties [20] such as nonlinear magnetic-field decay, imperfections in the magnetic and electric fields, and relativistic effects were calculated and found to be smaller than the statistical uncertainty by one to three orders of magnitude. Since ion-ion interactions may shift the measured cyclotron frequency [25], the average detected count rate was kept below one detected ion per spill (0.6–0.9 and for  $^{32-34}\text{Al}^+$  less than 0.1). Nonetheless, we performed a count-class analysis [26], in which the cyclotron frequency was linearly extrapolated to one trapped ion in MPET. The slopes were consistent with zero. The ratios calculated with the extrapolated frequencies were compared to ratios determined from data limited to 1–2 detected ions per spill and found to agree. Therefore, no corrections were made for ion-ion interactions for the mass measurements of radioisotopes. Systematic checks with stable ions were performed, and these frequency determinations were intermittently included during the measurements of  $^{30-34}\text{Al}^+$ :  $^{39}\text{K}^+$  when  $\text{O}_2^+$  was the reference ion and  $^{41}\text{K}^+$  when  $^{39}\text{K}^+$  was. These measurements agreed within  $1\sigma$  with the Atomic Mass Evaluation 2012 (AME'12) values for  $^{32-34}\text{Al}$  and within  $2\sigma$  for  $^{30,31}\text{Al}$ . To be conservative, we added the difference of the measured

TABLE I. Each Al isotope is listed with its half-life  $T_{1/2}$ , parameters for its measurement (reference ion, excitation time  $T_{RF}$ , Birge ratio  $R_{\text{Birge}}$  [10], and number of measurements  $N$ ), frequency ratio, measured mass excess  $\Delta_{\text{TITAN}}$ , evaluated mass excess  $\Delta_{\text{AME}}$  [6] (for  $^{29,32}\text{Al}$  AME'11 values [11] are given since TITAN values were included in AME'12), and the difference in mass excesses. For the ratio, the statistical uncertainty is listed in parentheses, followed by the systematic in parentheses and the total in square brackets. The  $^{27}\text{Al}$  ratio is the weighted average of five data sets. All ions were singly charged.

	$T_{1/2}$	Ref.	$T_{RF}$ [ms]	$R$	$R_{\text{Birge}}$	$N$	$\Delta_{\text{TITAN}}$ [keV]	$\Delta_{\text{AME}}$ [keV]	Diff. [keV]
$^{27}\text{Al}$	stable	$^{23}\text{Na}^+$		0.8520525329[17]	0.98	72	-17196.884(58)	-17196.75(10)	-0.14(12)
$^{29}\text{Al}$	6.56 min	$^{16}\text{O}_2^+$	97	1.103843599(46)(45)[65]	0.93	3	-18209.0(1.9)	-18215.4(1.2)	-6.3(1.6)
$^{30}\text{Al}$	3.62 s	$^{39}\text{K}^+$	96	1.29953346(7)(12)[18]	0.80	4	-15864.8(2.9)	-15872(14)	8(14)
$^{31}\text{Al}$	644 ms	$^{39}\text{K}^+$	76	1.25754941(5)(81)[12]	0.71	5	-14950.7(2.2)	-14955(20)	4(20)
$^{32}\text{Al}$	33 ms	$^{16}\text{O}_2^+$	47	1.00005455(2)(7)[24]	1.08	5	-11099.4(8.7)	-11062(86)	-37(86)
$^{33}\text{Al}$	42 ms	$^{39}\text{K}^+$	47	1.18104787(2)(19)[27]	0.90	6	-8497.4(7.0)	-8470(80)	-30(80)
$^{34}\text{Al}$	56 ms	$^{39}\text{K}^+$	47	1.14610193(26)(2)[26]	0.94	5	-2990.0(7.2)	-3070(70)	80(70)

and AME'12 frequency ratios in quadrature to the statistical uncertainty of the Al ratios.

For  $^{27}\text{Al}$ , the mass measurement was performed off line, with  $^{23}\text{Na}^+$  as the reference ion. Five sets of data were collected over several days. An excitation time of  $T_{RF} = 97$  ms was used once and  $T_{RF} = 997$  ms three times. For the final set we employed the Ramsey TOF-ICR excitation scheme [27], where the RF excitation was applied in two 200 ms pulses separated by 597 ms. We calculated the systematic error due to all sources mentioned above and added them in quadrature to the statistical uncertainty. The weighted average is given in Table I.

The measured Al mass excesses are summarized in Table I. For stable  $^{27}\text{Al}$ , we measured a 140 eV deviation from AME'12 and agree with a 2008 Penning-trap mass measurement [28]. For radioactive  $^{30,31,33,34}\text{Al}$ , the TITAN values agree with AME'12 although they are one order of magnitude more precise. As the TITAN values for  $^{29,32}\text{Al}$  are included in AME'12, their measured values are compared to the earlier AME'11 [11]. Our measurement of  $^{29}\text{Al}$  indicates the nuclide is 6 keV less bound than suggested by the 2011

TABLE II. Two-neutron separation energies  $S_{2n}$  (in MeV) for Mg and Al isotopes predicted in large-scale shell-model calculations (Th) from the Strasbourg-Madrid group are compared to experimental values (Exp) taken from this work and Ref. [6]. Excellent agreement is found between theory and the TITAN(-based) values, as can be seen in Fig. 3.

$N$	Mg		Al	
	Th	Exp	Th	Exp
16	14.84	14.9468(20)	16.86	17.148(2)
17	12.19	12.159(11)	14.94	15.157(1)
18	10.59	10.008(4)	13.30	12.889(1)
19	9.00	8.662(12)	11.36	11.377(7)
20	8.43	8.088(5)	9.57	9.689(5)
21	8.16	8.058(4)	8.01	8.033(10)
22	6.50	6.990(29)	7.58	7.865(70)
23	5.56	5.47(18)	8.02	7.20(10)
24	3.93	4.09(46)	6.15	6.11(14)
25	3.02		5.04	5.88(27)

reference value, based predominantly on one ( $t, p$ ) reaction [29], and supports earlier, less precise ( $\alpha, p$ ) determinations [30,31]. The TITAN  $^{32}\text{Al}$  value is in agreement with AME'11 and ten times more precise. The unprecedented precision in the mass values of  $^{32,34}\text{Al}$ , 9 and 7 keV respectively, allows for the first observation of a  $S_{2n}$  crossover.

Figure 1 depicts the  $S_{2n}$  values for the elements around the island of inversion, from oxygen ( $Z = 8$ ) to calcium ( $Z = 20$ ), and as shown in the inset, at  $N = 21$ , the Mg and Al values cross. Earlier hints at the crossover, e.g., as calculated from AME'03 [32], were obscured by the large uncertainties and spread of the  $^{31,33}\text{Mg}$  and  $^{32,34}\text{Al}$  TOF mass determinations. Subsequent measurements of the same type eliminated the crossover by more than  $1\sigma$  [11]. Yet, with the Penning-trap mass measurements of this work and Ref. [8] (where the  $N = 20$  shell gap was indeed discovered to have almost disappeared), the crossover has been clearly identified:  $S_{2n}(^{33}\text{Mg}) - S_{2n}(^{34}\text{Al}) = 24.8(10.8)$  keV. Everywhere else on the chart of nuclides, the difference  $S_{2n}(N, Z) - S_{2n}(N, Z + 1)$  is negative.

The source of the crossover is not immediately transparent. Due to its inclusion in the island of inversion and its even  $Z$ , the Mg isotopes have been the subject of detailed studies (see, e.g., Refs. [33,34] and references therein). Recent  $\gamma$ -ray spectroscopy [35] indicates the merging of the islands of shell breaking at  $N = 20$  and 28. Large-scale (i.e.  $N\hbar\Omega$ ) shell-model calculations from the Strasbourg-Madrid group indicate the deformation extends still further to  $N = 30$  [36]. These calculations have been continued in this work to predict the binding energies of the Mg and Al isotopes. They are compared to experimental values in Table II and Fig. 3.

For the Mg chain, excellent agreement is achieved between predictions and experimental values. The flattening for  $^{31-33}\text{Mg}$  reflects the large increase in correlation energy of these nuclei relative to the  $N - 2$  isotopes. For the odd- $Z$  Al isotopes, these calculations are the first detailed study of their island-of-inversion behavior and agree with the experimental data. Indeed, the only significant disagreement between the calculations and the experiment is for  $^{36}\text{Al}$ . The  $N\hbar\Omega$  calculations indicate that the  $S_{2n}$  trend flattens for  $^{34-36}\text{Al}$ , similar to that for  $^{31-33}\text{Mg}$ . From this slope we conclude that  $^{32-34}\text{Al}$  ( $19 \leq N \leq 21$ ) are *not* part of the island of

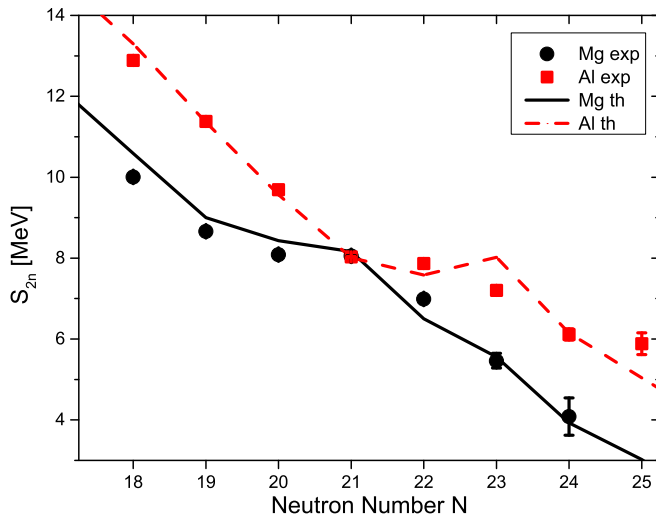


FIG. 3. (Color online) The two-neutron separation energy  $S_{2n}$  for the Mg and Al isotopes. The experimental values are taken from this work and [6]. The lines are the calculated values in the  $sd$ - $pf$  valence space.

inversion. Maximal correlation energy occurs around  $^{36}\text{Al}$ , and it is enough to put  $^{35-37}\text{Al}$  on the very edge of—if not part of—the island of inversion. The AME'12 value for  $^{36}\text{Al}$  is based on TOF mass measurements [6] and lies between the  $0\hbar\Omega$  and  $N\hbar\Omega$  predictions.

The origin of the crossover is better explained in Fig. 4. In the upper panel we have plotted the difference between the  $S_{2n}$ 's calculated with and without neutron excitations across  $N = 20$ . For the Mg isotopes the threshold effect of the entrance into the island of inversion is evident:  $^{32,33}\text{Mg}$  gain more correlation energy than  $^{30,31}\text{Mg}$  respectively.  $^{34}\text{Mg}$  is indeed inside the island of inversion, but its correlation energy gain is only 700 keV larger than that of  $^{32}\text{Mg}$ . The same argument explains why the values become negative beyond  $N = 22$ . The situation for the Al chain is much smoother because most of the isotopes are outside or, at most, at the edge of the island of inversion. The lower panel represents the difference of the two upper curves, showing the appearance of a majestic peak at  $N = 21$ , exactly where the crossover takes place. The curve also explains the narrowing of the gap between the two  $S_{2n}$  curves in Fig. 3 from  $N = 18$  to  $N = 21$  and the widening of the gap beyond  $N = 21$ . All in all, the explanation of this remarkable and unique crossover by the dominance of the deformed intruder configurations in the Mg isotopes appears very robust.

For completeness, we consider a very simple, complementary explanation. If an isomer had been delivered to the experiment with or instead of the ground state, whereupon the measured mass had been assigned to the ground state, the measured value would be higher than the ground-state mass. This was investigated [37]. No evidence was found for the delivery of a known isomer for  $^{31,33}\text{Mg}$  or  $^{32,34}\text{Al}$ ; the measured state was consistent with the accepted ground state in all cases. For  $^{34}\text{Al}$  we paid particular attention to the possibility of measuring the recently discovered  $1^+$  state [38]. Not only was there no evidence for a second species in any

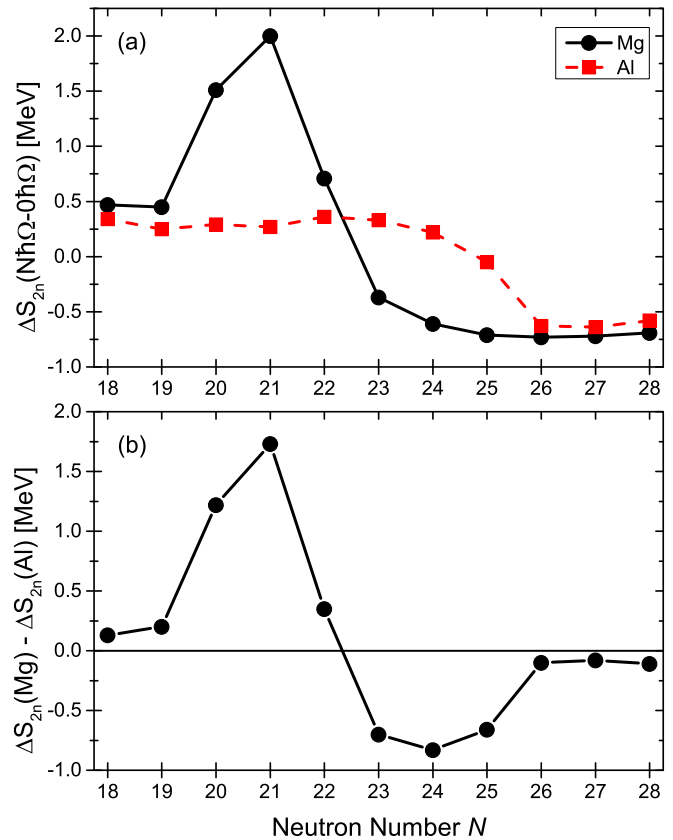


FIG. 4. (Color online) (a) Contribution of the neutron excitations outside of the  $sd$  shell to the two-neutron separation energies  $S_{2n}$  for the Mg and Al isotopes and (b) the relative values as a function of  $N$ .

$^{34}\text{Al}^+$  resonance (e.g., two resonances in Fig. 2), but also the count rate observed for the  $\approx 100$  ms measurement cycle was consistent with the 56 ms accepted ground state [39] and inconsistent with the 26 ms state [38]. Moreover, an isomer would result in a smaller effect than the gain in correlation energy discussed above.

In summary, we have measured the masses of the neutron-rich Al isotopic chain ( $A = 27, 29-34$ ) with Penning-trap mass spectrometry. Good agreement with previous literature values has been found for all isotopes, but the order-of-magnitude improvement in precision has uncovered a previously unobserved phenomenon: An unexpected crossover in the  $S_{2n}$  has been found at  $N = 21$ . This is the only known occurrence of a crossover on the  $S_{2n}$  surface. Large-scale shell-model calculations show that the crossover is a threshold effect associated with the entrance into the  $N = 20$  island of inversion of the neutron-rich Mg isotopes.

We appreciate support from the TRILIS group led by J. Lassen, the ISAC Beam Delivery group, M. Good, M. R. Pearson, and D. Frekers. This work has been supported by the Natural Sciences and Engineering Research Council (NSERC) of Canada and the National Research Council (NRC) of Canada through TRIUMF and by the French INP3 project PICS06207. A.T.G. acknowledges support from the NSERC CGS-D, A.L. from the Deutsche Forschungsgemeinschaft

(DFG) under Grant No. FR601/3-1, T.D.M from NSERC CGS-M, T.J.M.R. from the DAAD RISE Internship 2013, and V.V.S. from the Studienstiftung des deutschen Volkes.

A.P. is supported by MINECO (Spain) (FPA2011-29854) and Centro de Excelencia Severo Ochoa SEV-2012-0249 grants.

- 
- [1] M. G. Mayer, *Phys. Rev.* **75**, 1969 (1949); O. Haxel, J. Jensen, and H. Suess, *ibid.* **75**, 1766 (1949).
- [2] C. Thibault, R. Klapisch, C. Rigaud *et al.*, *Phys. Rev. C* **12**, 644 (1975).
- [3] Y. Blumenfeld, T. Nilsson, and P. Van Duppen, *Phys. Scr.* **152**, 014023 (2013).
- [4] O. Sorlin and M. G. Porquet, *Prog. Part. Nucl. Phys.* **61**, 602 (2008), and references therein; K. Heyde and J. L. Wood, *Rev. Mod. Phys.* **83**, 1467 (2011).
- [5] A. Poves and J. Retamosa, *Phys. Lett. B* **184**, 311 (1987); E. K. Warburton, J. A. Becker, and B. A. Brown, *Phys. Rev. C* **41**, 1147 (1990).
- [6] G. Audi, M. Wang, A. H. Wapstra, F. G. Kondev, M. MacCormick, X. Xu, and B. Pfeiffer, *Chin. Phys. C* **36**, 1287 (2012).
- [7] Z. Meisel and S. George, *Int. J. Mass Spec.* **349**, 145 (2013).
- [8] A. Chaudhuri, C. Andreoiu, T. Brunner, U. Chowdhury, S. Ettenauer, A. T. Gallant, G. Gwinner, A. A. Kwiatkowski, A. Lennarz, D. Lunney *et al.*, *Phys. Rev. C* **88**, 054317 (2013).
- [9] R. W. Ibbotson, T. Glasmacher, B. A. Brown *et al.*, *Phys. Rev. Lett.* **80**, 2081 (1998).
- [10] R. Birge, *Phys. Rev.* **40**, 207 (1932).
- [11] G. Audi and W. Meng (private communication).
- [12] J. Dilling, R. Baartman, P. Bricault, M. Brodeur, L. Blomeley, F. Buchinger, J. Crawford, J. R. Crespo López-Urrutia, P. Delheij, M. Froese *et al.*, *Int. J. Mass Spectrom.* **251**, 198 (2006).
- [13] K. Blaum, J. Dilling, and W. Nörtershäuser, *Phys. Scr.* **152**, 014017 (2013).
- [14] M. Brodeur, T. Brunner, C. Champagne, S. Ettenauer, M. Smith, A. Lapierre, R. Ringle, V. Ryjkov, S. Bacca, P. Delheij *et al.*, *Phys. Rev. Lett.* **108**, 052504 (2012).
- [15] M. Smith, M. Brodeur, T. Brunner, S. Ettenauer, A. Lapierre, R. Ringle, V. Ryjkov, F. Ames, P. Bricault, G. Drake *et al.*, *Phys. Rev. Lett.* **101**, 202501 (2008).
- [16] S. Ettenauer, M. C. Simon, A. T. Gallant, T. Brunner, U. Chowdhury, V. V. Simon, M. Brodeur, A. Chaudhuri, E. Mané, C. Andreoiu *et al.*, *Phys. Rev. Lett.* **107**, 272501 (2011).
- [17] V. V. Simon, T. Brunner, U. Chowdhury, B. Eberhardt, S. Ettenauer, A. T. Gallant, E. Mané, M. C. Simon, P. Delheij, M. R. Pearson *et al.*, *Phys. Rev. C* **85**, 064308 (2012).
- [18] J. Lassen, P. Bricault, M. Dombbsky, J. P. Lavoie, C. Geppert, and K. Wendt, in *LASER 2004*, edited by Z. Blaszcak, B. Markov, and K. Marinova (Springer-Verlag, Berlin, 2006), pp. 69–75.
- [19] T. Brunner, M. J. Smith, M. Brodeur, S. Ettenauer, A. T. Gallant, V. V. Simon, A. Chaudhuri, A. Lapierre, E. Mané, R. Ringle *et al.*, *Nucl. Instrum. Meth. A* **676**, 32 (2012).
- [20] M. Brodeur, V. L. Ryjkov, T. Brunner, S. Ettenauer, A. T. Gallant, V. V. Simon, M. J. Smith, A. Lapierre, R. Ringle, P. Delheij *et al.*, *Int. J. Mass Spectrom.* **310**, 20 (2012).
- [21] T. Brunner, A. R. Mueller, K. O’Sullivan, M. C. Simon, M. Kossick, S. Ettenauer, A. T. Gallant, E. Mané, D. Bishop *et al.*, *Int. J. Mass Spectrom.* **309**, 97 (2011).
- [22] M. König, G. Bollen, H. J. Kluge, T. Otto, and J. Szerypo, *Int. J. Mass Spectrom.* **142**, 95 (1995).
- [23] G. Gräff, H. Kalinowsky, and J. Traut, *Z. Phys. A-Hadron Nucl.* **297**, 35 (1980).
- [24] G. Bollen, R. B. Moore, G. Savard, and H. Stolzenberg, *J. Appl. Phys.* **68**, 4355 (1990).
- [25] ISOLDE Collaboration, G. Bollen, H. J. Kluge, M. König, T. Otto, G. Savard, H. Stolzenberg, and G. Audi, *Phys. Rev. C* **46**, R2140 (1992).
- [26] A. Kellerbauer, K. Blaum, G. Bollen, F. Herfurth, H. J. Kluge, M. Kuckein, E. Sauvan, C. Scheidenberger, and L. Schweikhard, *Eur. Phys. J. D* **22**, 53 (2003).
- [27] S. George, K. Blaum, F. Herfurth, A. Herlert, M. Kretzschmar, S. Nagy, S. Schwarz, L. Schweikhard, and C. Yazidjian, *Int. J. Mass Spectrom.* **264**, 110 (2007).
- [28] S. George, G. Audi, B. Blank *et al.*, *Europhys. Lett.* **82**, 50005 (2008).
- [29] M. S. Antony, J. Britz, J. Bueb, and A. Pape, *Nuovo Cimento A* **81**, 414 (1984).
- [30] H. Graetzer and A. Robbins, *Phys. Rev.* **105**, 1570 (1957).
- [31] R. Bearse, D. Youngblood, and J. Yntema, *Phys. Rev.* **167**, 1043 (1968).
- [32] G. Audi, A. H. Wapstra, and C. Thibault, *Nucl. Phys. A* **729**, 337 (2003).
- [33] D. T. Yordanov, M. L. Bissell, K. Blaum *et al.*, *Phys. Rev. Lett.* **108**, 042504 (2012).
- [34] N. A. Smirnova, K. Heyde, B. Bally, F. Nowacki, and K. Sieja, *Phys. Rev. C* **86**, 034314 (2012).
- [35] P. Doornenbal, H. Scheit, S. Takeuchi *et al.*, *Phys. Rev. Lett.* **111**, 212502 (2013).
- [36] E. Caurier, F. Nowacki, and A. Poves, *Phys. Rev. C* **90**, 014302 (2014).
- [37] A. T. Gallant, M. Brodeur, T. Brunner *et al.*, *Phys. Rev. C* **85**, 044311 (2012).
- [38] F. Rotaru, F. Negoita, S. Grévy *et al.*, *Phys. Rev. Lett.* **109**, 092503 (2012).
- [39] S. Nummela, P. Baumann, E. Caurier *et al.*, *Phys. Rev. C* **63**, 044316 (2001).